Decadal Climate Simulations Using Accurate and Fast Neural Network Emulation of Full, Long- and Short Wave, Radiation

Vladimir M. Krasnopolsky,

SAIC at NCEP/NOAA, and

Earth System Science Interdisciplinary Center, University of Maryland

Michael S. Fox-Rabinovitz, and Alexei A. Belochitski,

Earth System Science Interdisciplinary Center, University of Maryland

Corresponding author address:
Vladimir Krasnopolsky,
5200 Auth Rd.,
Camp Springs, MD 20746-4304;
Phone: 301-763-8000 x 7262, Fax: 301-763-8545,
E-mail: Vladimir.Krasnopolsky@noaa.gov

Revised version submitted to Monthly Weather Review

December 2007

Abstract

Approach to calculating model physics using neural network emulations, previously proposed and developed by the authors, has been implemented in this study for both long-wave and short-wave radiation parameterizations, or to the *full model radiation*, the most time-consuming component of model physics. The developed highly accurate neural network emulations of the NCAR CAM (Community Atmospheric Model) long-wave and short-wave radiation parameterizations are 150 and 20 times faster than the original/control long-wave and short-wave radiation parameterizations, respectively. The full neural network model radiation was used for a decadal climate model simulation with the NCAR CAM. A detailed comparison of parallel decadal climate simulations performed with the original NCAR model radiation parameterizations and with their neural network emulations is presented. Almost identical results have been obtained for the parallel decadal simulations. It opens the opportunity of using efficient neural network emulations for the full model radiation for decadal and longer climate simulations as well as for weather prediction.

1. Introduction

One of the main problems in development and implementation of state-of-the-art numerical climate and weather prediction models is the complexity of physical processes involved. Some of the model physics parameterizations, such as radiation, are time-consuming even for most powerful modern supercomputers, and because of that are calculated less frequently than other model physics components and model dynamics. This may negatively affect the accuracy of a model's physics calculation and its temporal consistency which may, in turn, reduce the accuracy of climate simulations and weather predictions.

The calculation of model physics in GCM (General Circulation Model) used in this study, the NCAR (National Center for Atmospheric Research) CAM (Community Atmospheric Model), with the T42 (~3 degree) horizontal resolution and 26 vertical levels (T42L26), takes about 70% of the total model computations. Evidently, this percentage is model dependent but full model radiation is the most time-consuming component of GCMs (e.g., Morcrette et al. 2007a,b). Such a situation is an important motivation for looking for new alternative numerical algorithms that provide faster calculations of model physics while carefully preserving their accuracy. We used the NCAR CAM with the climatological sea surface temperature forcing for the study as a testbed available to the community for experimentation.

During the last decade new emerging neural network (NN) techniques have found a variety of applications in different fields and, more specifically, to accurate and fast

modeling of atmospheric radiative processes (*Krasnopolsky 1997, Chevallier et al. 1998*) and for satellite retrieval procedures (e.g., *Krasnopolsky, 1997; Krasnopolsky and Schiller, 2003*). The NN techniques have been successfully applied to development of a new long-wave radiation (LWR) parameterization ("NeuroFlux") for the ECMWF (European Centre for Medium-range Weather Forecasting) model (*Chevallier et al. 1998, 2000*). NeuroFlux, which is 8 times faster than the previous parameterization, consists of a battery of about 40 neural networks. NeuroFlux has been used operationally within the ECMWF 4-DVAR (4-dimensional variational) data assimilation system since October 2003.

A new approach based on the application of a statistical learning technique (NNs) to *emulation* of model physics parameterizations has been introduced to ocean models (*Krasnopolsky et al. 2000, 2002, Tolman et al. 2004*), and recently applied by the authors to the NCAR CAM-2 atmospheric physics parameterizations (*Krasnopolsky et al. 2005*). A new type of GCM, the hybrid GCM (HGCM), has also been introduced (*Krasnopolsky and Fox-Rabinovitz, 2006 a, b*). HGCM is based on a synergetic combination of statistical learning and deterministic model components. The approach uses a particular kind of statistical or machine learning technique, NNs, for accurate and fast *emulation* of model physics components. The term "emulation" means a complete, accurate, and robust functional imitation of the input/output relationship or mapping that exists between input and output vectors of model physics parameterizations (Krasnopolsky 2007).

NN emulations are developed for the *existing*, i.e., original parameterizations of atmospheric physics. This allows us to preserve the integrity and the level of sophistication of the state-of-the-art physical parameterizations of atmospheric processes. Due to the capability of modern statistical learning techniques to provide an unprecedented accuracy for emulations of complex, multidimensional, and multi-scale systems like model physics, our NN emulations of model physics parameterizations are practically identical to the original physical parameterizations in terms of the functional input/output relationship. They are usually significantly (one to five orders of magnitude) faster than the original parameterizations (Krasnopolsky et al. 2002, 2005). In other words*, the underlying idea of the approach is not to develop a new parameterization but rather to emulate a parameterization already carefully tested and validated by its developers.* This is achieved by using data for NN training simulated by an atmospheric model run with the original parameterization. Using model-simulated data for NN training allows us to achieve an unprecedented accuracy of the approximation because simulated data are free of the problems typical for empirical data (like a high level of observational noise, sparse spatial and temporal coverage, poor representation of extreme events, etc.). The accuracy and speed-up of NN emulations is always measured against the original parameterization. The developed NN emulation has the same inputs and outputs as the original parameterization, which allows us to use it as a functional substitute for the original parameterization.

The key objective of this study is validating the efficiency of developed NN emulations for the NCAR CAM full radiation block in terms of a close similarity of decadal climate

simulations using the original radiation parameterizations (for the control simulation) and their NN emulations.

In the study, we apply the NN approach to approximating both the LWR and short-wave radiation (SWR) parameterizations in the NCAR CAM (*e.g., Journal of Climate, 1998*). Calculation of the LWR and SWR or the full/total model radiation is the most time consuming part of the atmospheric physics calculations. For example, the NCAR CAM T42 total radiation (LWR and SWR) takes ~70% of the time required for calculation of model physics. Because calculation of model physics takes about 70% of the total model computations, the calculation of T42L26 full radiation takes ~50% of the total model calculation time. A description of NN emulations for LWR in the NCAR CAM and results of their use in 10-year climate simulations with the model are provided in *Krasnopolsky et al. (2005)*. Also, the NN emulations for LWR and SWR are discussed in *Krasnopolsky and Fox-Rabinovitz (2006 a, b)*. In this study, we will concentrate on a discussion of the results of a decadal (50 year) NCAR CAM climate simulation using NN emulations simultaneously for both LWR and SWR, i. e., for their combined application as the full model radiation. The model simulation using the combined NN emulations is compared with or actually validated against the control model simulation using the original LWR and SWR parameterizations.

In Section 2, the NN approach and developed NN emulations for NCAR CAM LWR and SWR are briefly described in terms of their design, accuracy, and computational performance. In Section 3, the results of the two parallel decadal model simulations, one

using the combined LWR and SWR NN emulations for full model radiation and the other using the original model radiation (the control) are compared in terms of closeness of their spatial and temporal variability characteristics. Section 4 contains conclusions.

2. NN emulations for the NCAR CAM radiation

2.1 Background Information on NN emulations for LWR and SWR

NN emulations of model physics are based on the following considerations. Any parameterization of model physics can be formulated as a continuous or almost continuous mapping (input vector vs. output vector dependence) and can be symbolically written as:

$$Y = M(X); \quad X \in \Re^n, Y \in \Re^m \tag{1}$$

where M denotes the mapping, n is the dimensionality of the input space (the number of NN inputs), and m is the dimensionality of the output space (the number of NN outputs). NNs (multilayer perceptrons, in our case) are a generic tool for approximation of such mappings (Funahashi 1989, Hornik 1991).

NN is an analytical approximation that uses a family of functions like:

$$y_q = a_{q0} + \sum_{j=1}^{k} a_{qj} \cdot \phi(b_{j0} + \sum_{i=1}^{n} b_{ji} \cdot x_i); \quad q = 1,2,\ldots,m \tag{2}$$

where x_i and y_q are components of the input and output vectors X and Y, respectively, a and b are fitting parameters, and $\phi(b_{j0} + \sum_{i=1}^{n} b_{ji} \cdot x_i)$ is a "neuron". The activation function ϕ is usually a hyperbolic tangent, n and m are the numbers of inputs and outputs,

respectively, and k is the number of neurons in the hidden layer. Definitions of NN terminology can be found in many places, for example in the recent book by Bishop (2006) and in Krasnopolsky (2007); however, eq. (2) is sufficient to understand the subject of this paper.

The major goals for developing NN emulation for model physics are to obtain an extremely high accuracy for NN emulation with practically zero biases or systematic errors. This is a necessary condition for obtaining non-accumulating errors during long-term climate simulations with developed NN emulations. The choice of an optimal version of NN emulation is based on accuracy, not on a speed-up of computation. All the NN emulations obtained provide a very significant speed-up anyway. The most efficient and convenient way of developing NN emulations for model physics components is to develop a single NN for a model physics parameterization. Such an approach has been introduced and discussed in Krasnopolsky et al. *(2005)* and Krasnopolsky and Fox-Rabinovitz (*2006 b*).

The LWR and SWR parameterizations together comprise the full model radiation. The LWR and SWR parameterizations or the *full model radiation* have been emulated using NNs in the NCAR CAM-2. The function of the radiation (LWR and SWR) parameterizations in atmospheric GCMs is to calculate radiation fluxes and heating rates produced by the LWR and SWR atmospheric processes. The complete description of NCAR CAM atmospheric LWR and SWR parameterizations is presented by *Collins (2001, 2002*). A very general and schematic outline of these parameterizations, in order

to illustrate the complexity that makes them a computational bottleneck in the NCAR CAM physics, is given in *Krasnopolsky and Fox-Rabinovitz (2006 b)*.

The input vectors for the NCAR CAM-2 LWR parameterization include ten profiles (atmospheric temperature, humidity, ozone, CO_2, N_2O, CH_4, two CFC mixing ratios (the annual mean atmospheric mole fractions for the halocarbons), pressure, cloud emissivity, and cloud cover) and one relevant surface characteristic (the upward LWR flux at the surface). The LWR parameterization output vectors consist of the profile of heating rates (HRs) and several radiation fluxes, including the outgoing LW radiation flux from the top layer of the model atmosphere (the outgoing LWR or OLR).

The NN emulation of the LWR parameterization has exactly the same inputs (total 220 inputs; $n = 220$ in eq. (1)) and the same outputs (total 33 outputs; $m = 33$ in eq. (1)) as the original LWR parameterization. *Krasnopolsky et al. (2005)* have developed several NNs, all of which have one hidden layer with 20 to 300 neurons ($k = 20$ to 300 in eq. (2)). Varying the number of hidden neurons allows us to demonstrate the dependence of the accuracy of approximation on this parameter as well as its convergence, and as a result, provide a sufficient accuracy of approximation for the climate model.

The input vectors for the SWR parameterization include twenty one vertical profiles (specific humidity, ozone concentration, pressure, cloud cover, layer liquid water path, liquid effective drop size, ice effective drop size, fractional ice content within cloud., aerosol mass mixing ratios, etc.), solar zenith angle and surface albedo for four different

bands. The SWR parameterization output vectors consist of a vertical profile of heating rates (HRs) and several radiation fluxes. The NN emulations of the SWR parameterization have 173 inputs and 33 outputs. We have developed several NNs, all of which have one hidden layer with 50 to 200 neurons (k = 50 to 200 in eq. (2)).

It is noteworthy that the number of NN inputs is less then the number of input profiles multiplied by the number of the vertical layers plus the number of relevant single level characteristics. Many input variables (e.g., all gases) have zero or constant values in upper vertical layers. These constant values are not included as NN inputs because NN does not need constants inputs.

The NCAR CAM-2 (T42L26) was run for two years to generate representative data sets. The representative data set adequately samples the atmospheric state variability. The first year of simulation was divided into two independent parts, each containing input/output vector combinations. The first part was used for training and the second for tests (control of overfitting, control of NN architecture, etc.). The second year of simulation was used to create a validation data set completely independent of both the training and test data sets. The third part or the validation set was used for validations only. All approximation statistics presented in this section are calculated using this independent validation data set. The accuracy of the NN run, i.e., biases and rmse, are calculated against the control run.

2.2 Bulk Approximation Error Statistics

To ensure a high quality of representation of the LWR and SWR radiation processes, the accuracy of the NN emulations has been carefully investigated. Our NN emulations have been validated against the original NCAR CAM LWR and SWR parameterizations. To calculate the error statistics presented in Table 1 and the following figures of this section, the original parameterizations and their NN emulations have been applied to a validation data set. Two sets of the corresponding HR profiles have been generated for both LWR and SWR. Total and level bias (or mean error), total and level RMSE, profile RMSE or PRMSE, and σ_{PRMSE} have been calculated (*Krasnopolsky et al., 2005*, *Krasnopolsky and Fox-Rabinovitz 2006a*). Some of these statistics presented in Table 1 have been calculated as follows. The outputs of the original parameterization and the NN emulations can be represented as: $Y(i,j)$ and $Y_{NN}(i,j)$, respectively, where $i = (lat, lon)$, $i=1,\ldots,N$ is the horizontal location of a vertical profile, N is the number of horizontal grid points, and $j = 1,\ldots, L$ is the vertical index where L is the number of vertical levels.

The mean difference, B (bias or a systematic error of approximation), between the original parameterization and its NN emulation, is calculated as follows:

$$B = \frac{1}{N \times L} \sum_{i=1}^{N} \sum_{j=1}^{L} [Y(i,j) - Y_{NN}(i,j)] \tag{2}$$

The root mean square error has been calculated for each ith profile:

$$prmse(i) = \sqrt{\frac{1}{L} \sum_{j=1}^{L} [Y(i,j) - Y_{NN}(i,j)]^2} \tag{2}$$

This error can be used to calculate mean profile root mean square error, *PRMSE*, and its standard deviation, σ_{PRMSE}:

$$PRMSE = \frac{1}{N}\sum_{i=1}^{N} prmse(i)$$
$$\sigma_{PRMSE} = \sqrt{\frac{1}{N-1}\sum_{i=1}^{N}[prmse(i) - PRMSE]^2} \quad (3)$$

Table 1 shows bulk validation statistics for the accuracy of approximation and computational performance for the best (in terms of accuracy and performance) developed NN emulations: NN 50 (k = 50 hidden neurons in eq.(2)) for the LWR emulation and NN 55 (k = 55 hidden neurons in eq.(2)) for the SWR emulation. The errors profiles for LWR and SWR are shown in Fig. 4 of *Krasnopolsky (2007)*. The NN emulations developed for LWR and SWR are highly accurate. They have practically zero bias and a quite small PRMSE. Zonal mean differences between the NN emulation and the original parameterization for radiative fluxes at the top of the atmosphere and at the surface have also been produced. The differences appear to be uniformly small for all latitudes, mostly within ±0.5 W/m^2 and do not exceed ±1 W/m^2.

The NN emulations using 50 neurons in the hidden layer provide, if run *separately* at every model physics time step (1 hour), a speed-up of roughly 150 times for LWR and 20 times for SWR as compared with the original LWR and SWR, respectively. It is noteworthy that the main reason for the smaller performance gain for NN SWR vs. NN LWR is that the original CAM SWR parameterization is simpler and about 10 times faster than the original CAM LWR.

Using NN emulations *simultaneously* for LWR and SWR or for the full model radiation results in an overall significant, 13-fold acceleration of calculations for the entire/full

model radiation block. It is worth clarifying, for a better understanding of the overall speed-up, that for the usual control run the original LWR (including time-consuming optical properties calculations) is calculated less frequently, only every 12 hours or twice a day, and only computationally inexpensive heating rates and radiative fluxes are calculated every hour. Notice that all other inputs, including cloud cover, which is represented by a vertical profile of cloud fraction, are updated hourly. For the model run using NN emulations, LWR (including both optical properties and heating rates and radiative fluxes) is calculated more frequently, every hour, consistent with SWR and other model physics calculations. We also performed an additional costly control run with the original LWR calculated every hour, as it is done in the LWR NN run, for a limited period (10 years). The results of the two control runs appeared to be very close. The difference between them is significantly less than the difference between each of them and the LWR NN run. Because of that we decided to validate the 40 year full radiation NN run against the usual control run.

3. Validation of parallel decadal model simulations

The comparisons between diagnostic and prognostic fields for the relatively short parallel model runs, one using the original LWR or SWR (the control run) and the other one using NN emulations for the LWR or SWR parameterizations, are presented in *Krasnopolsky at al. (2005)*, and in *Krasnopolsky and Fox-Rabinovitz (2006 a,b)*. They show that the parallel runs produce the results that are close to each other. Therefore, both components of radiation, LWR and SWR, can be successfully emulated using the NN approach.

These results opened the opportunity to use both NN emulations, for LWR and SWR (or full model radiation) simultaneously, in a multi-decadal simulation using NCAR CAM (T42L26), the results of which are discussed below. The results of multi-decadal climate simulations performed with NN emulations for both LWR and SWR, i. e., for the full model radiation, have been validated against the parallel control NCAR CAM simulation using the original LWR and SWR. Below we estimate closeness of the results for these parallel 50-year climate simulations. Note that the first 10 years of simulations are not included in the validation to avoid the impact of spin-up effects, so that years 11-50 are used for the validation. The spin-up is done for the original NCAR CAM; it is not related to the use of NN emulations. We will analyze below the differences between the parallel runs in terms of time and spatial (global) means as well as temporal characteristics.

Table 2 presents comparisons between the parallel control and NN emulation runs in terms of the time (40-year) and global mean characteristics and the differences between the results of the parallel runs. Basically, the differences, in terms of mean, rms,

minimum and maximum characteristics, between the parallel runs, are small. More specifically, there are negligible mean differences (bias), 0.02 hPa and -0.1 K, in sea level pressure and 2-meter temperature, respectively, between the NN and control runs. For these fields, rmse, minimum and maximum differences are also small. Other time and global mean differences presented in Table 2, including such sensitive fields as total precipitation, total cloud amount, cloud amounts for high, low, and mid clouds, total grid-box cloud liquid and ice water paths, top of model net long-wave flux and cloud forcing, also show a close similarity, in terms of all presented difference characteristics, between the parallel simulations for these fields. These differences are within typical observational and reanalysis errors/uncertainties. Note that minimum and maximum differences in Table 2 are not averaged in space and time but rather are instantaneous grid point values obtained for the entire 40-year simulation.

Let us discuss the differences between the parallel simulations in terms of spatial and temporal characteristics. Zonal and time mean heating (or cooling) rates for LWR and SWR are presented in Figs. 1 and 2, respectively. The HR patterns (the upper panels) are practically indistinguishable and their differences (the bottom panels) are small. It confirms that the NN emulations for LWR and SWR are very close to their original parameterizations throughout the model simulations. It is noteworthy that the HR differences in SWR and especially in LWR are a bit larger at the surface because HRs are larger there (Figs. 1 and 2). For the zonal means it is not easy to distinguish between the ocean and land. However, the differences seem to be larger over the mountainous Antarctica region (60º S to 90º S) as well as over the Northern Hemisphere mid-latitudes

where the major mountains are located (such as those in Europe, Asia and North America).

Fig. 3 shows a very close similarity in zonal and time mean 2-meter temperature for the parallel simulations (the upper panel) where their differences are within the -0.6 K to 0.3 K range (the bottom panel).

The zonal and time mean vertical distributions of temperature for the parallel runs (Fig. 4) are close to each other and their difference or mean bias is practically zero, with minimum and maximal biases within ~ 2-2.5 K by magnitude. This larger zonal bias occurs in the stratosphere mostly over the Southern polar domain. However, it is comparable with typical observational and/or reanalysis errors/uncertainties (just as a reference) and also comparable with the differences between the NCEP and ECMWF reanalysis.

Close similarities have also been obtained for the results of parallel runs in terms of time mean spatial fields such as 850 hPa temperature presented in Fig. 5. The horizontal fields presented in the upper and middle panels are close to each other. For the difference field (the bottom panel), bias is negligible (-0.06 K), RMSE is small (0.34 K), and minimum and maximum values (~-1.6 K and ~0.9 K) are well within observational or reanalysis errors/uncertainties.

In addition to global distributions such as shown in Fig. 5 it is important to assess the

differences between the parallel simulations at a local (station) level, an example of which is presented in Fig. 6. The vertical distributions of time mean temperature are very close for both runs at the local level as well.

Now we compare the results of the parallel simulations in terms of temporal characteristics. Fig. 7 shows the winter-summer differences for time mean temperature at 850 hPa. Their patterns are practically indistinguishable and the minimum and maximum values are very close. The global mean time series for time mean temperature at 850 hPa presented in Fig. 8 are very similar throughout the entire decadal simulations for the parallel runs, with only occasional small differences (within 0.5 K) that are well below the observation and reanalysis errors. The annual cycle for global mean temperature at 850 hPa is presented in Fig. 9. It shows very small differences between the runs, with the maximum within 0.2 K for January. The precipitation annual cycles are very close for both runs (the upper panels) and their differences or bias (the bottom panel) is quite small. Close similarity has also been obtained for other model prognostic and diagnostic fields in term of their spatial and temporal characteristics.

The results obtained confirm the profound similarity in parallel climate simulations, which justifies the possibility of using efficient neural network emulations of full model radiation for decadal and longer climate simulations as well as for weather prediction models. The methodology developed can be applied to other LWR and SWR schemes used in a variety of models, process studies, and other applications.

4. Conclusions

In this study, we presented an approach based on a synergetic combination of deterministic modeling based on physical (first principle) equations and statistical learning (NN emulation) components within an atmospheric model. The statistical learning approach was used to develop highly accurate and fast NN emulations for model physics components. Here we presented a NN emulation of the full atmospheric radiation, i.e. for long- and short-wave radiation parameterizations used in numerical climate and weather prediction models.

This study has shown the practical possibility of using highly efficient NN emulations for the full model radiation block for decadal (50 year) climate simulations. A very high accuracy and increased speed of NN emulations for the NCAR CAM full radiation (LWR and SWR) has been achieved. The systematic errors introduced by NN emulations of full model radiation are negligible and do not accumulate during the decadal model simulation. The random errors of NN emulations are also small as is shown in Section 2. Almost identical results have been obtained for the parallel 50-year climate simulations as shown in Section 3. These results show the potential of developing efficient NN emulations for model physics components and the entire model physics.

The NN emulation approach presented here is very robust. It was applied to both LWR and SWR parameterizations in different models with different dynamical cores and with different resolutions. For example, in addition to the NCAR CAM applications presented here, this approach was applied to the NASA NSIPP model and to the NCEP CFS model,

using NN emulations of the LWR parameterizations (Krasnopolsky and Fox-Rabinovitz 2006 a, Krasnopolsky et al. 2008). In all these cases, the systematic errors introduced by NN emulations are negligible and the random errors are very small, similar to errors presented in this paper. The computational speed-ups achieved in all these cases are also similar (about two orders of magnitude).

Applying the NN emulation approach, which allows such a significant speed-up with preservation of the accuracy and functional integrity of the model physics, may create some challenges that can be resolved using the tremendous flexibility of statistical learning techniques and of the NN technique in particular. Because NN emulations are statistical approximations, there exists a small probability of larger approximation errors or outliers. These larger errors can be successfully controlled using a compound parameterization technique with a quality control procedure for removing larger errors (Krasnopolsky 2007) or using the NN ensemble approach with NN emulations (Fox-Rabinovitz et al. 2006). The NN emulation technique is sensitive to the resolution of the model used, especially to vertical resolution, which determines the NN emulation architecture, i.e., the number of inputs and outputs. Every time the vertical resolution of the model is changed, the NN emulation needs to be retrained. It is noteworthy that NN retraining can be done routinely and takes a limited time and effort once the practical framework for a specific model is developed.

As mentioned above, the NN emulations described in this study have been developed only for the *existing* model parameterizations. Extension of the NN-approach to

developing new *parameterizations* goes beyond the scope of this study and could be done as a collaborative effort with parameterization developers interested in implementation of more sophisticated and realistic model physics, which are now computationally prohibitive. Also, it is noteworthy that the NN emulation technique can be applied to accelerate calculations of the model chemistry.

MMAB Contribution No. 258

Acknowledgments. The authors would like to thank Drs. W. Collins, P. Rasch, J. Tribbia (NCAR), F. Baer, and D. Chalikov (University of Maryland) for useful discussions and consultations. This study is based upon the work supported by the NOAA/CDEP/CTB grant NA06OAR4310047.

References

Bishop Ch. M., 2006: *Pattern Recognition and Machine Learning*. Springer, 738 pp.

Chevallier, F., F. Chéruy, N. A. Scott, and A. Chédin, 1998: A neural network approach for a fast and accurate computation of longwave radiative budget, *Journal of Applied Meteorology*, **37**, 1385-1397.

_____, J.-J. Morcrette, F. Chéruy, and N. A. Scott, 2000: Use of a neural-network-based longwave radiative transfer scheme in the EMCWF atmospheric model, *Quarterly Journal of Royal Meteorological Society*, **126**, 761-776.

Collins, W.D., 2001: Parameterization of generalized cloud overlap for radiative calculations in general circulation models, *J. Atmos. Sci.,* **58**, 3224-3242

_____, J.K. Hackney, and D.P. Edwards, 2002: An updated parameterization for infrared emission and absorption by water vapor in the National Center for Atmospheric Research Community Atmosphere Model*, J. Geophys. Res.,* **107** (**D22**), 1-20.

Fox-Rabinovitz M. S., V. Krasnopolsky, and A. Belochitski, 2006: Ensemble of Neural Network Emulations for Climate Model Physics: The Impact on Climate Simulations*, Proc., 2006 International Joint Conference on Neural Networks,* Vancouver, BC, Canada, July 16-21, IEEE, 9321-9326, CD-ROM

Funahashi, K. (1989). On the Approximate Realization of Continuous Mappings by Neural Networks. *Neural Networks*, **2**, 183-192.

Journal of Climate, 1998: v. 11, No. 6 (the special issue).

Hornik, K. (1991). Approximation Capabilities of Multilayer Feedforward Network. *Neural Networks*, 4, pp. 251-257.

Krasnopolsky, V.M., 1997: A neural network forward model for direct assimilation of SSM/I brightness temperatures into atmospheric models, in *Research Activities in Atmospheric and Oceanic Modeling*, CAS/JSC Working Group on Numerical Experimentation, Report No. 25, WMO/TD-No. 792, 1.29-1.30

_____, 2007: Neural Network Emulations for Complex Multidimensional Geophysical Mappings: Applications of Neural Network Techniques to Atmospheric and Oceanic Satellite Retrievals and Numerical Modeling, *Reviews of Geophysi*cs, in press

_____, and H. Schiller, 2003: Some neural network applications in environmental sciences. Part I: Forward and inverse problems in satellite remote sensing", *Neural Networks*, **16**, 321- 334

_____, and M.S. Fox-Rabinovitz, 2006a: A New Synergetic Paradigm in Environmental Numerical Modeling: Hybrid Models Combining Deterministic and Machine Learning Components, *Ecological Modelling*, 191, pp. 5–18.

_____, and M.S. Fox-Rabinovitz, 2006b: Complex hybrid models combining deterministic and machine learning components for numerical climate modeling and weather prediction, *Neural Networks* 19, 122–134.

_____, D. V. Chalikov, and H. L. Tolman, 2002: "A Neural Network Technique to Improve Computational Efficiency of Numerical Oceanic Models", *Ocean Modelling*, v.4, 363-383.

_____, M.S. Fox-Rabinovitz, and D.V. Chalikov, 2005: "Fast

and Accurate Neural Network Approximation of Long Wave Radiation in a Climate Model", *Monthly Weather Review*, vol. 133, No. 5, pp. 1370-1383.

_____, M.S. Fox-Rabinovitz, H.L. Tolman, and A. A. Belochitski, 2007: Neural Network Approach for Robust and Fast Calculation of Physical Processes in Numerical Environmental Models: Compound Parameterization with a Quality Control of Larger Errors, *Neural Networks*.

_____, M. S. Fox-Rabinovitz, Y. T. Hou, S. J. Lord, and A. A. Belochitski, 2008: Accurate and Fast Neural Network Emulations of Long Wave Radiation for the NCEP Climate Forecast System Model, *20th Conference on Climate Variability and Change*, New Orleans, January 2008.

Morcrette, J.-J., G. Mozdzynski and M. Leutbecher, 2007a: A reduced radiation grid for the ECMWF Integrated Forecasting System, ECMWF Technical Memorandum No. 538, September 21, 2007

_____, P. Bechtold, A. Beljaars, A. Benedetti, A. Bonet, F. Doblas-Reyes, J. Hague, M. Hamrud, J. Haseler, J.W. Kaiser, M. Leutbecher, G. Mozdzynski, M. Razinger, D. Salmond, S. Serrar, M. Suttie, A. Tompkins, A. Untch and A. Weisheimer, 2007b: Recent advances in radiation transfer parametrizations, ECMWF Technical Memorandum No. 539, October 18, 2007

Figure-caption list.

Fig. 1 Zonal and time mean LWR Heating Rates, in K/day, for the NN LWR run (the upper left panel), the control run (the upper right panel) and their difference (the bottom panel).

Fig. 2 Same as in Fig. 1 but for the SWR.

Fig. 3 Zonal and time mean 2-meter temperature, in K, for the full radiation NN and control runs (the upper panel) and their difference (the bottom panel).

Fig. 4 Zonal mean vertical distribution of time mean temperature, in K, for the full radiation NN run (the upper left panel), the control run (the upper right panel), and their difference or bias (the bottom panel).

Fig. 5 Time mean temperature at 850 hPa, in K, for the full radiation NN run (the upper panel), the control run (the middle panel), and their difference (the bottom panel).

Fig. 6 Vertical profile of time mean temperature, in K, at the Resolute, Canada station for the full radiation NN run (the dashed line), the control run (the solid line), and observations (the dotted line).

Fig. 7 Winter-summer difference for time mean temperature at 850 hPa, in K, for the full radiation NN run (the upper panel), and the control run (the bottom panel).

Fig. 8 Global mean time series for time mean temperature at 850 hPa, in K, for the full radiation NN run (the dotted line), and the control run (the solid line).

Fig. 9 Annual cycle for global mean temperature at 850 hPa, in K, for the full radiation NN run (the dashed line), and the control run (the solid line).

Fig. 10 Annual cycle for precipitation, in mm/day, for the full radiation NN run (the upper left panel), the control run (the upper right panel), and their difference or bias (the bottom panel).

Table 1. Statistics estimating the accuracy of HRs (in K/day) calculations and computational performance for NCAR CAM-2 LWR and SWR using NN emulation vs. the original parameterization.

	Bias (K/day)	**PRMSE (K/day)**	σ_{PRMSE} **(K/day)**	**Performance (times faster)**
LWR NN 50	$3. \cdot 10^{-4}$	0.28	0.20	150
SWR NN 55	$-4. \cdot 10^{-3}$	0.15	0.12	20

Table 2. Time (40-year) and global means for model diagnostics from NCAR CAM-2 control climate simulations with the original LWR and SWR, simulation with NN emulations for the full radiation using NN 50 (LWR) and NN 55 (SWR), and their differences. SLP – sea level pressure; T2M – temperature at 2 m ; U-200 - 200 hPa zonal wind; TPR - total precipitation rate; TCA - total cloud amount; HLCA - high-level cloud amount; LLCA - low-level cloud amount; MLCA - mid-level cloud amount; TGCLWP - total grid-box cloud liquid water path; TGCIWP - total grid-box cloud ice water path; TOMNLW - top of model net long-wave flux; TOMLWC - top of model long-wave cloud forcing.

Field	**Control**	**NN Full Radiation**	**Mean Difference**	**RMS Difference**	**Min Difference**	**Max Difference**
SLP (hPa)	1011.48	1011.50	0.02	0.52	-2.04	1.57
T2M (K)	287.37	287.27	- 0.1	0.26	-1.64	0.78
U-200 (m/s)	16.21	16.29	0.08	0.86	-2.31	3.95
TPR (mm/day)	2.86	2.89	0.03	0.2	-1.84	1.19
TCA (%)	60.71	61.12	0.41	1.42	-7.50	5.76
HLCA(%)	43.05	43.29	0.24	1.63	-7.52	8.01
LLCA(%)	31.67	31.93	0.26	1.06	-5.20	4.78
MLCA(%)	19.11	19.14	0.03	0.81	-4.86	4.39
TGCLWP (g/m^2)	60.23	60.59	0.36	3.02	-19.43	14.95
TGCIWP (g/m^2)	8.82	8.83	0.01	0.39	-1.69	1.45
TOMNLW (W/m^2)	234.48	234.54	0.06	2.32	-8.37	11.56
TOMLWC (W/m^2)	29.33	29.07	-0.26	2.45	-15.59	7.64

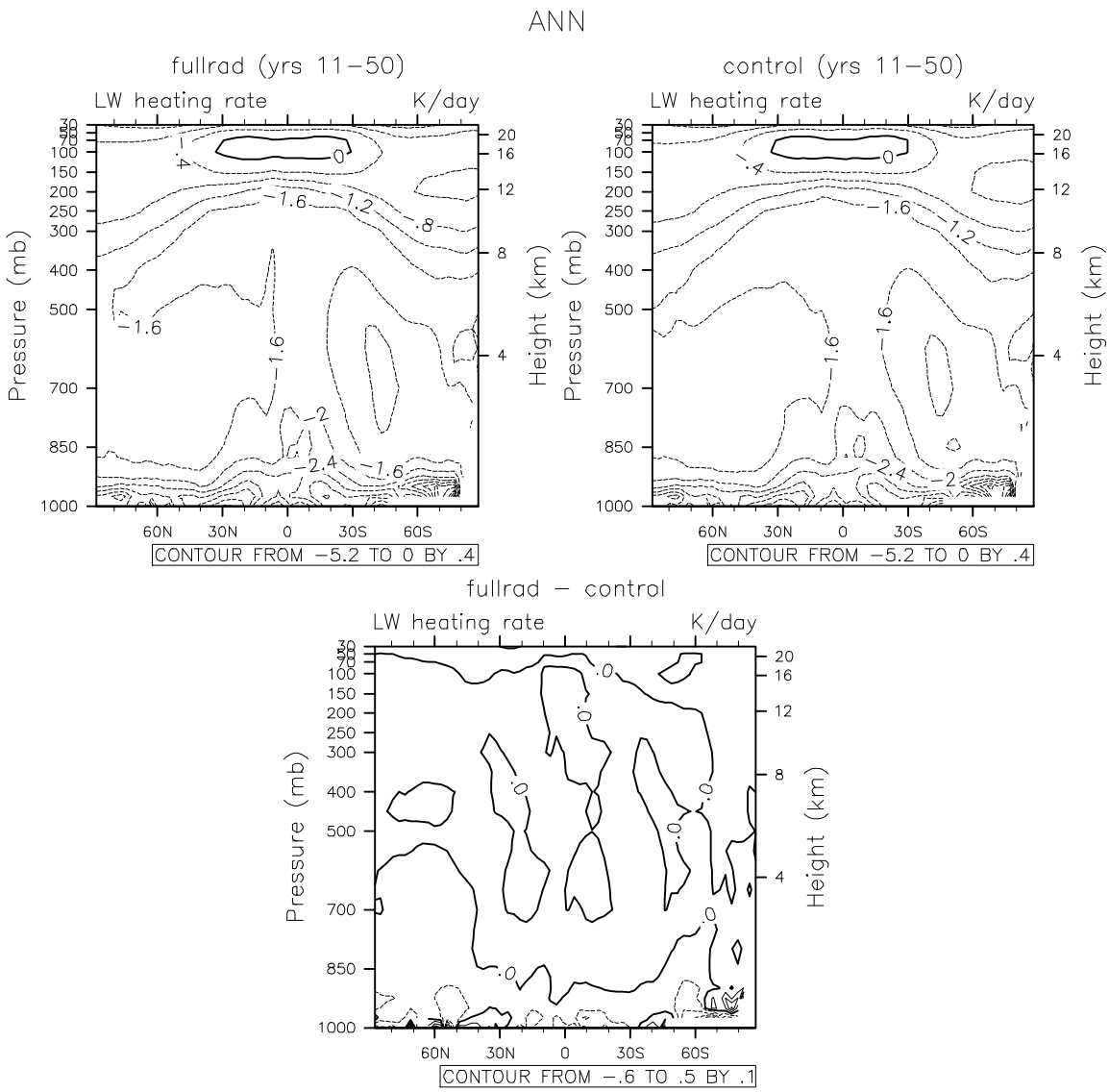

Fig. 1 Zonal and time mean LWR Heating Rates, in K/day, for the NN LWR run (the upper left panel), the control run (the upper right panel) and their difference (the bottom panel).

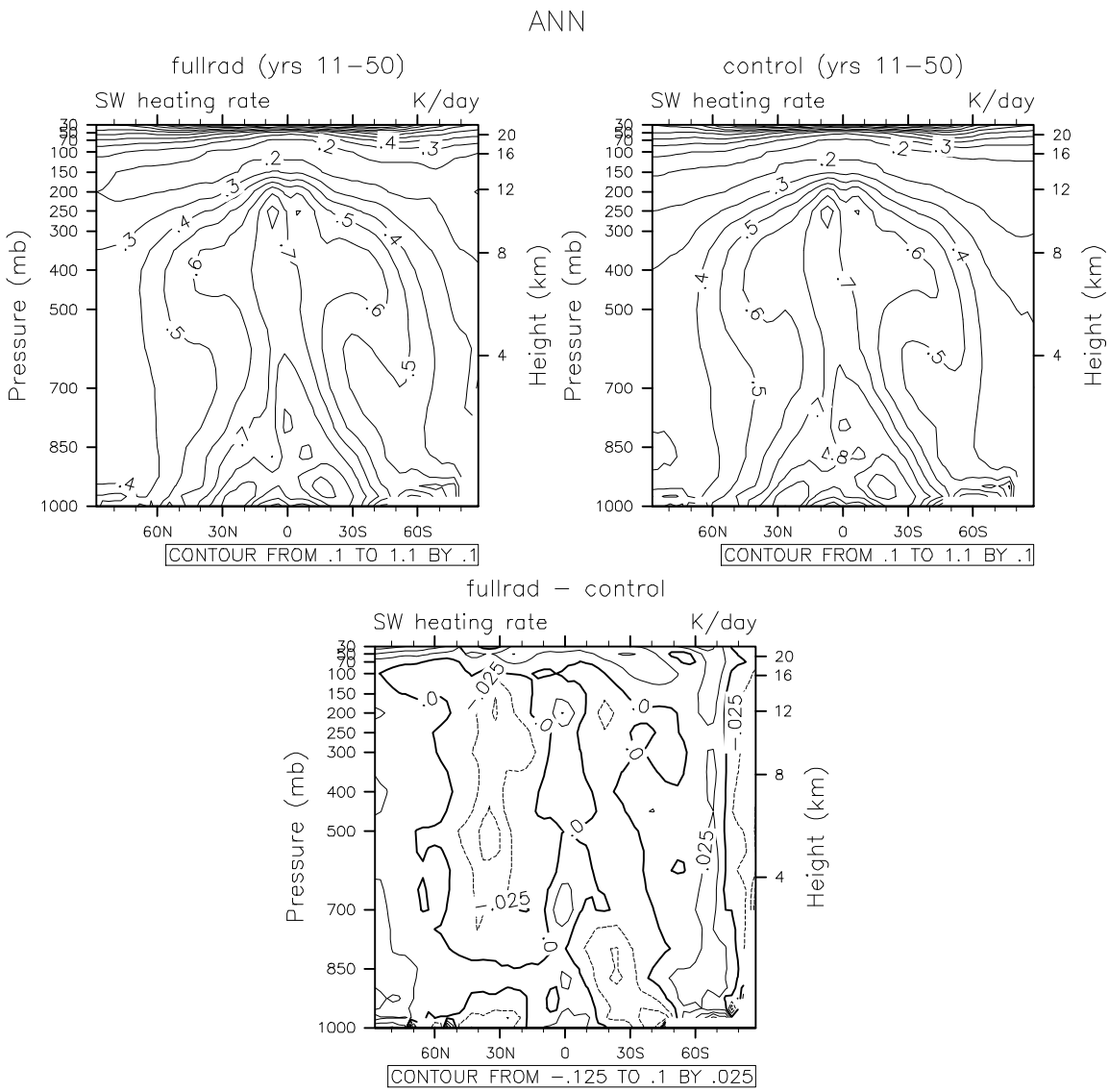

Fig. 2 Same as in Fig. 1 but for the SWR.

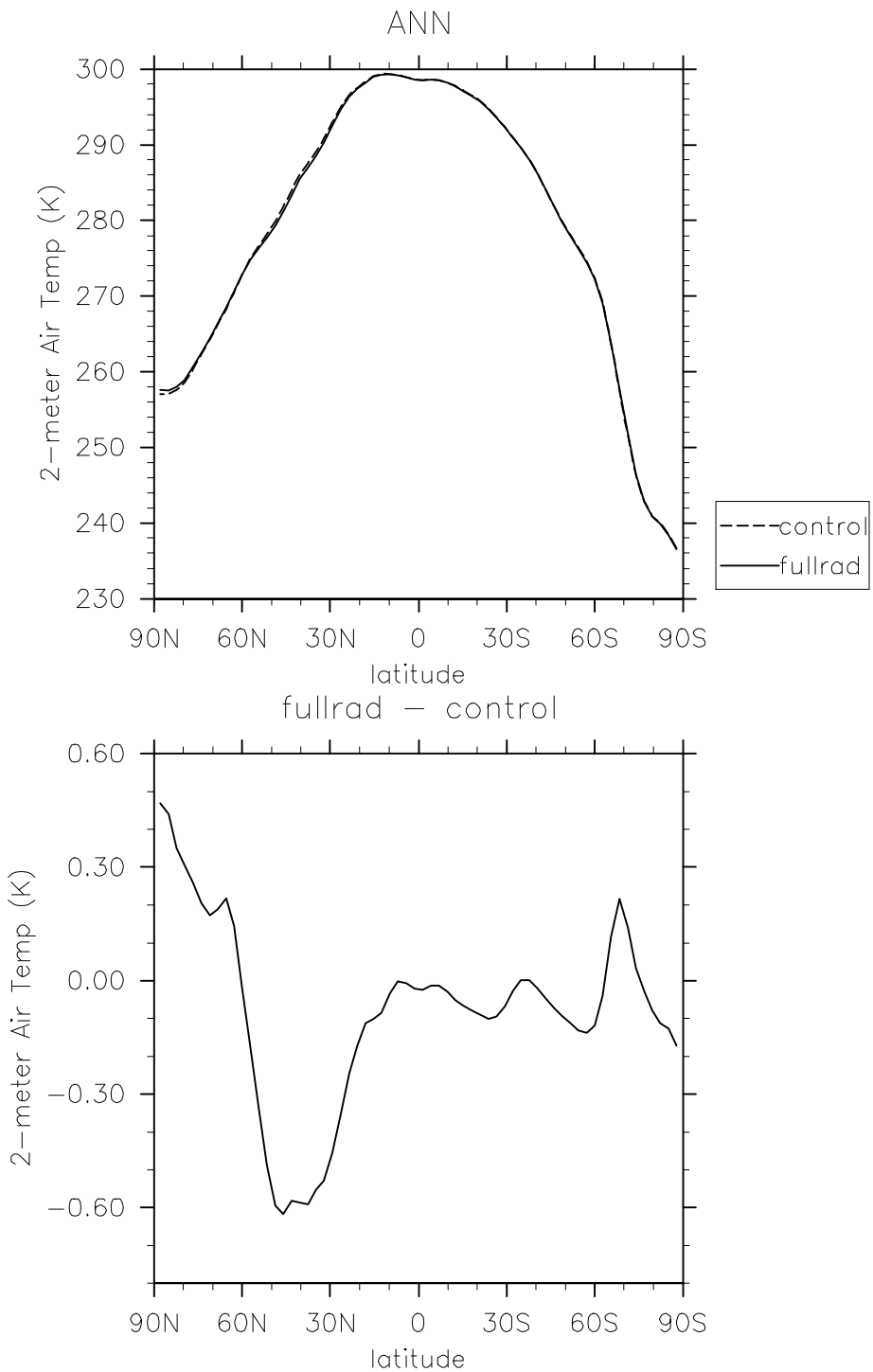

Fig. 3 Zonal and time mean 2-meter temperature, in K, for the full radiation NN and control runs (the upper panel) and their difference (the bottom panel).

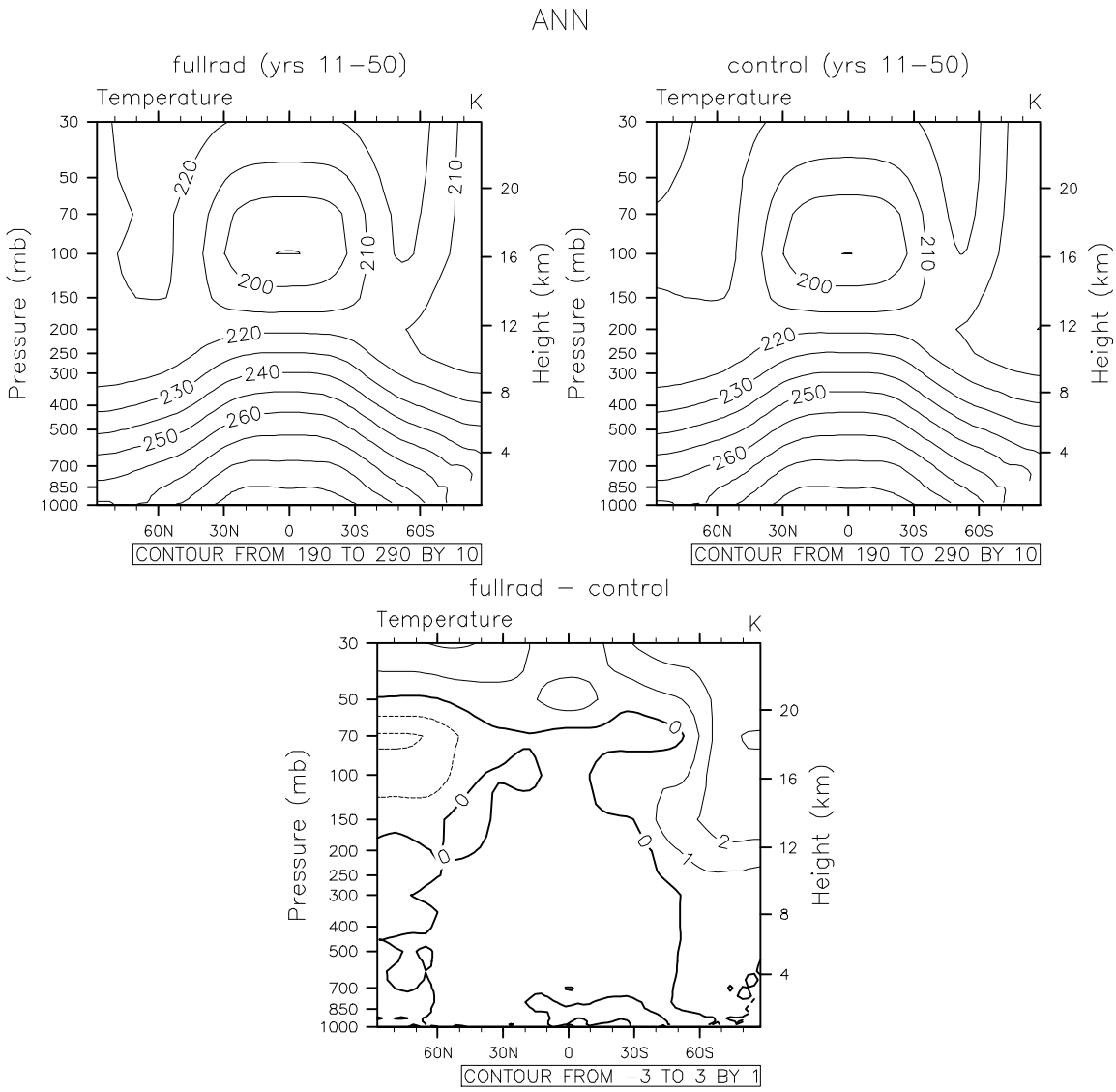

Fig. 4 Zonal mean vertical distribution of time mean temperature, in K, for the full radiation NN run (the upper left panel), the control run (the upper right panel), and their difference or bias (the bottom panel).

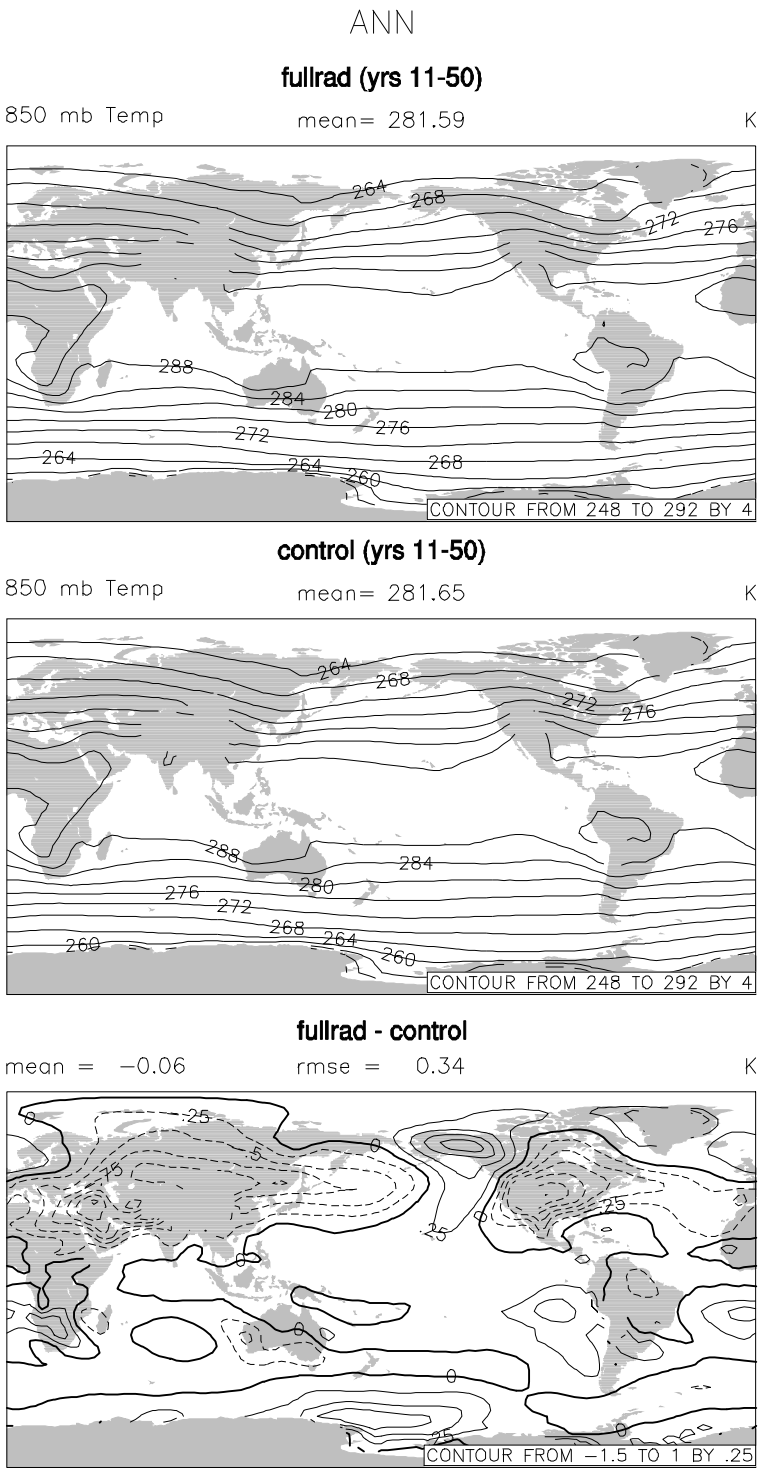

Fig. 5 Time mean temperature at 850 hPa, in K, for the full radiation NN run (the upper panel), the control run (the middle panel), and their difference (the bottom panel).

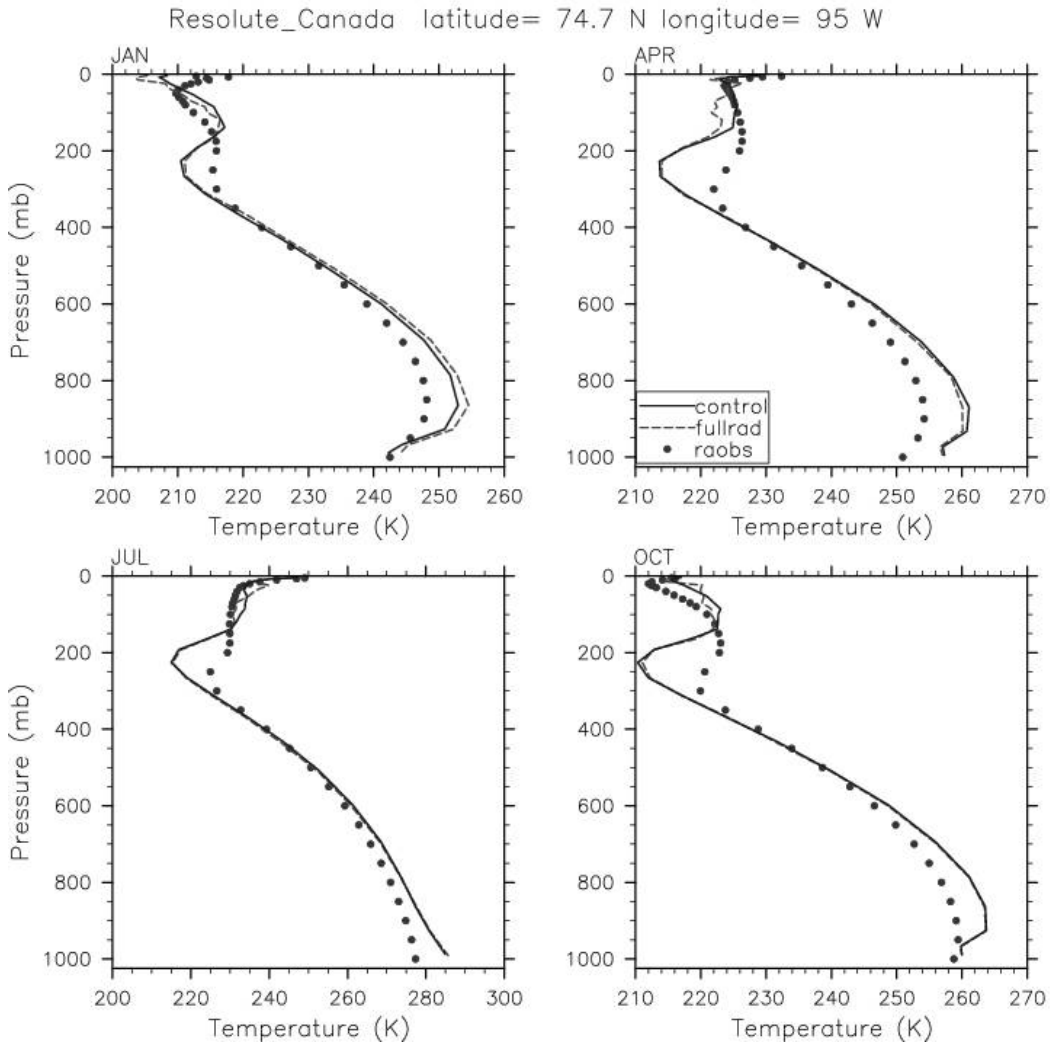

Fig. 6 Vertical profile of time mean temperature, in K, at the Resolute, Canada station for the full radiation NN run (the dashed line), the control run (the solid line), and observations (the dotted line).

DJF-JJA

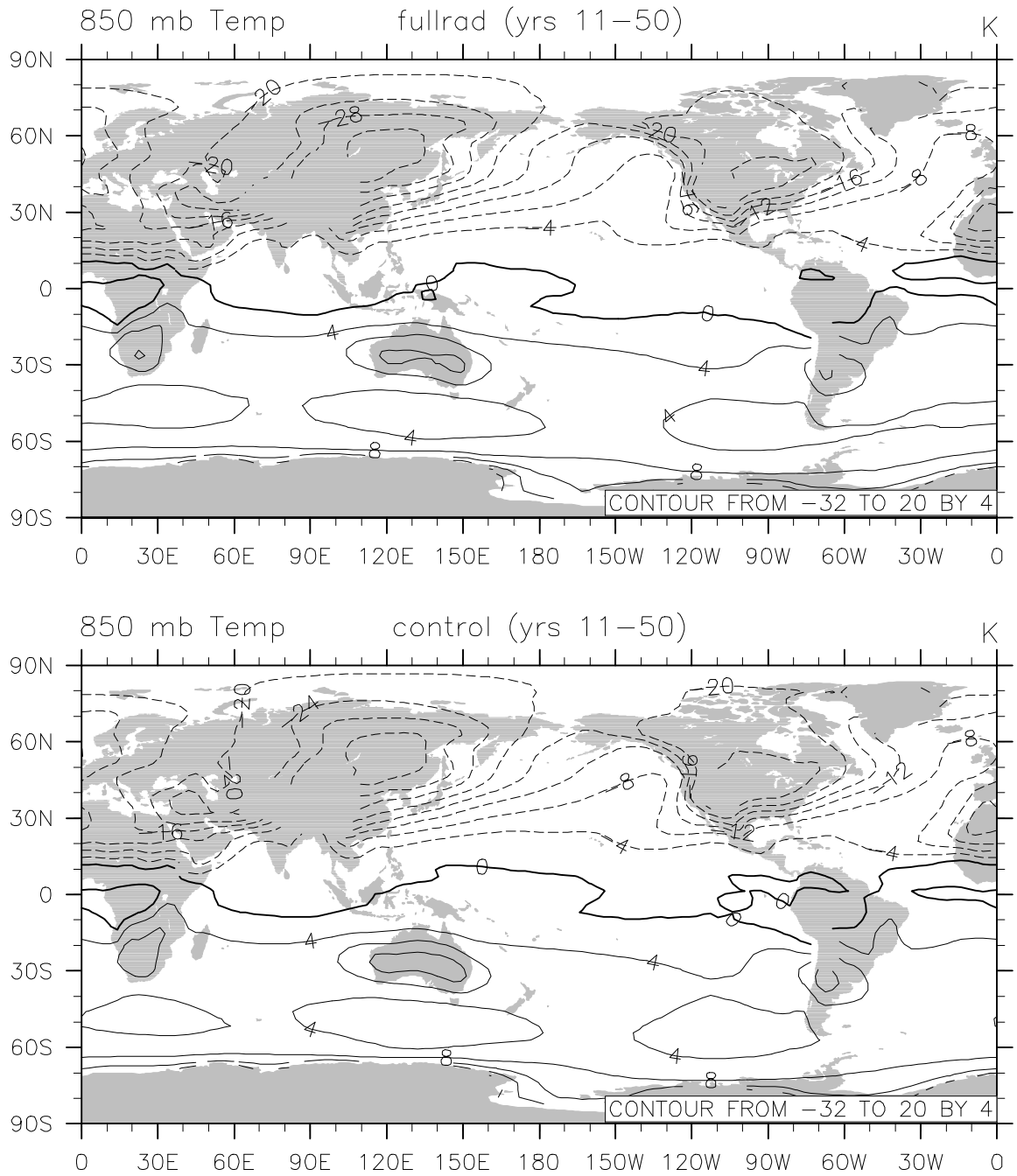

Fig. 7 Winter-summer difference for time mean temperature at 850 hPa, in K, for the full radiation NN run (the upper panel), and the control run (the bottom panel).

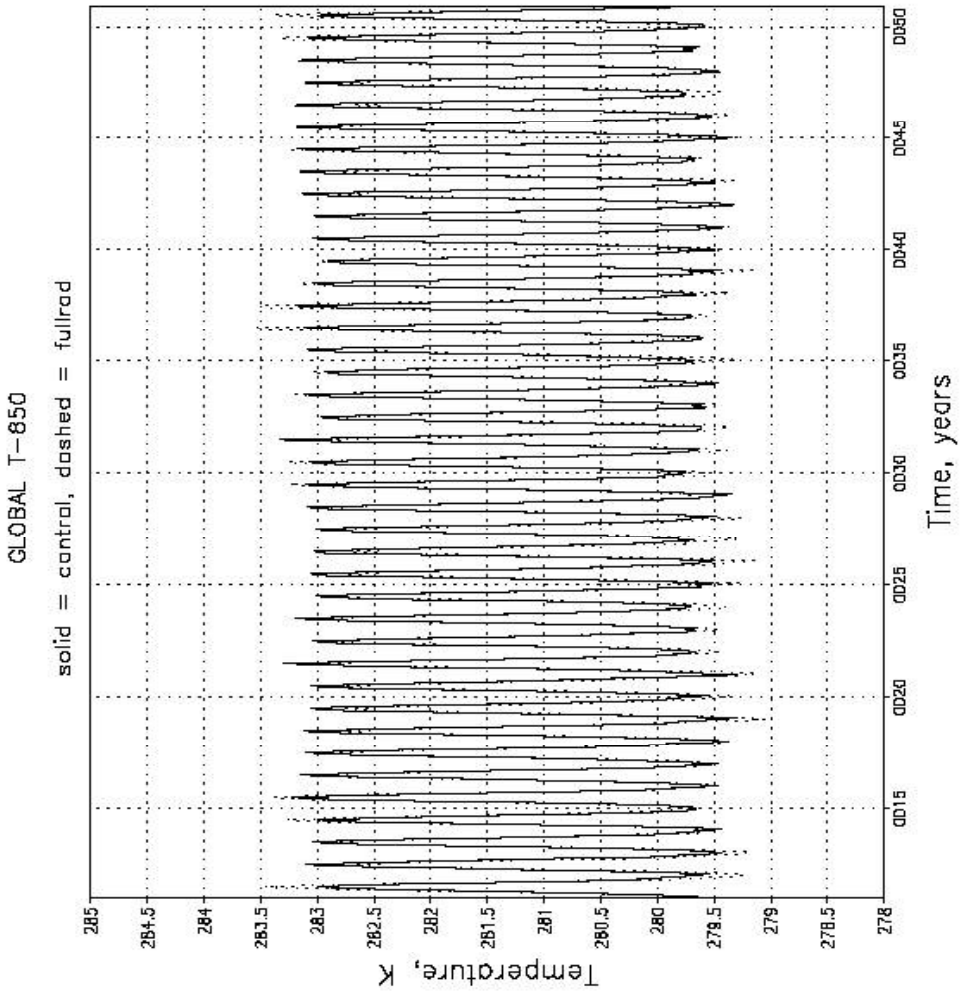

Fig. 8 Global mean time series for time mean temperature at 850 hPa, in K, for the full radiation NN run (the dotted line), and the control run (the solid line).

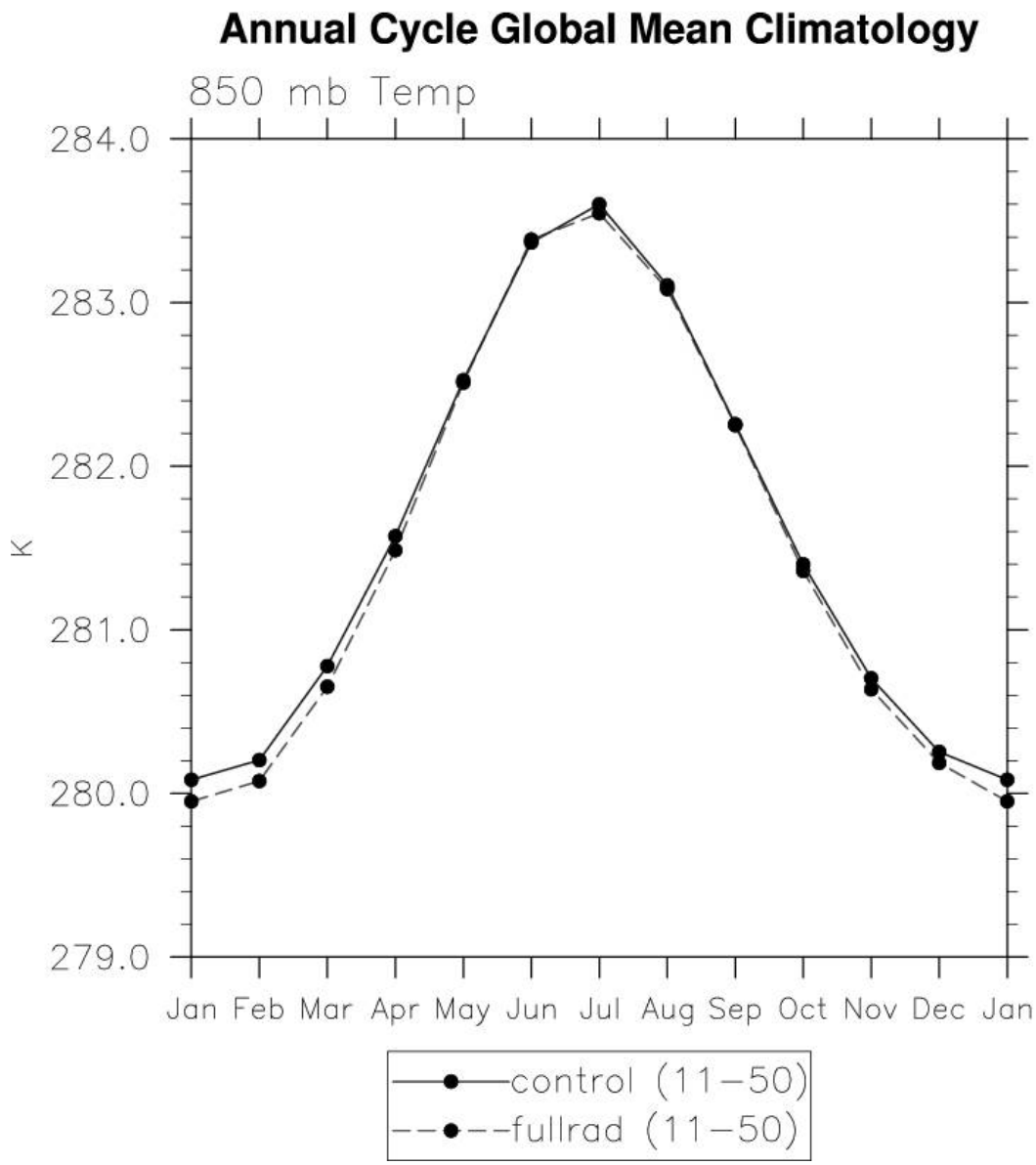

Fig. 9 Annual cycle for global mean temperature at 850 hPa, in K, for the full radiation NN run (the dashed line), and the control run (the solid line).

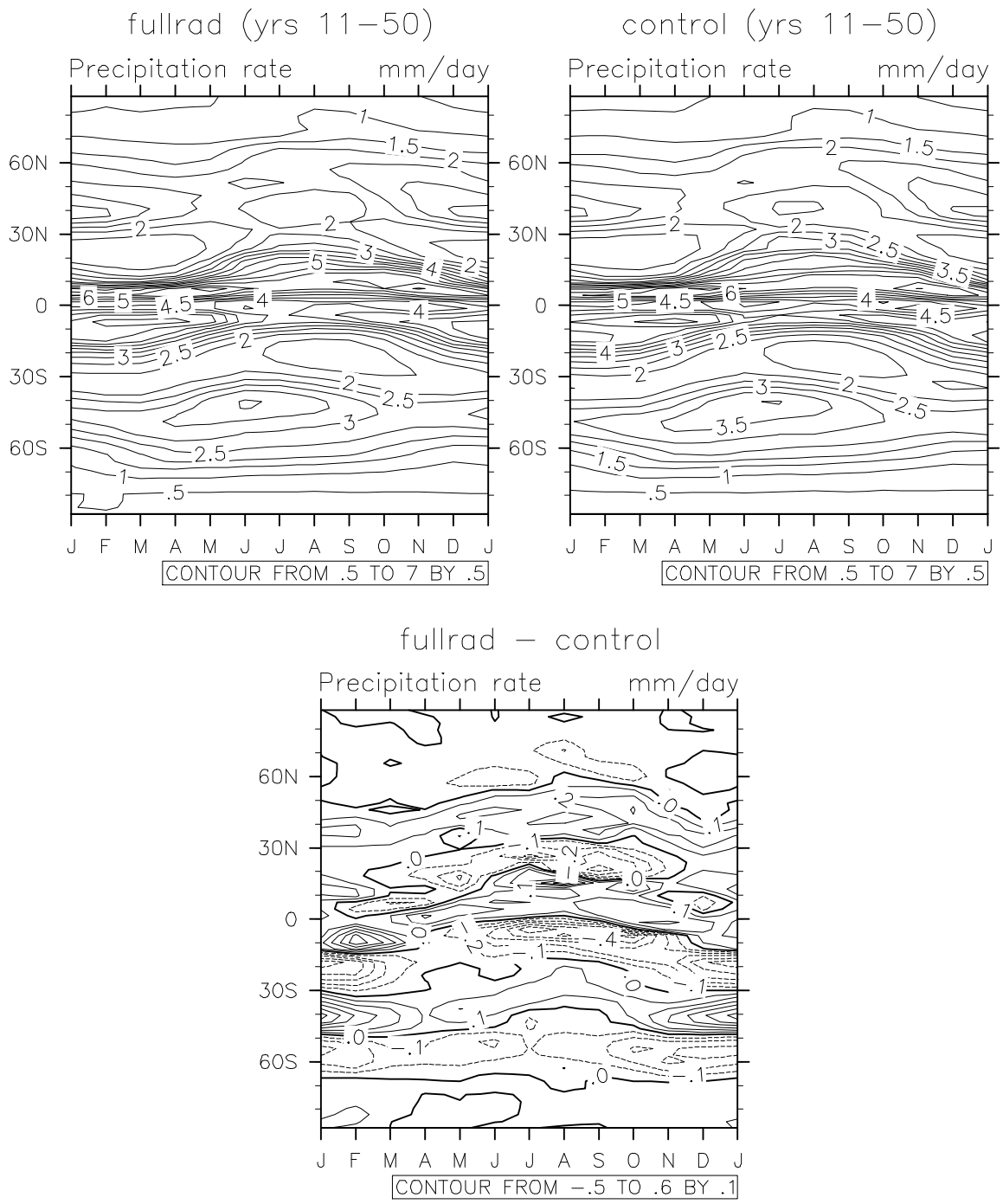

Fig. 10 Annual cycle for precipitation, in mm/day, for the full radiation NN run (the upper left panel), the control run (the upper right panel), and their difference or bias (the bottom panel).